ELSEVIER

Journal of Chromatography A 826 (1998) 87–94

JOURNAL OF CHROMATOGRAPHY A

Interface for the coupling of capillary electrophoresis and inductively coupled plasma mass spectrometry

Anders Tangen[a,*], Walter Lund[a], Bjørn Josefsson[b], Hans Borg[c]

[a]*Department of Chemistry, University of Oslo, P.O. Box 1033, N-0315 Oslo, Norway*
[b]*Department of Analytical Chemistry, Stockholm University, S-10691 Stockholm, Sweden*
[c]*ITM Solna, Stockholm University, S-10691 Stockholm, Sweden*

Received 6 April 1998; received in revised form 25 August 1998; accepted 25 August 1998

Abstract

The coupling of capillary electrophoresis and inductively coupled plasma (ICP) mass spectrometry is described using a new direct injection nebulizer designed for liquid flow-rates of 1–15 μl min^{-1} (aqueous solutions). The liquid flow-rate working range was found to depend on the nebulizer design. An extra flow of electrolyte was used to complete the electrical circuit. This design was found to work better than the conductive paint and crack hole designs. The CE–ICP-MS system was tested by analysing mixtures of alkali/alkaline earth metals and Cr(III)/Cr(VI), using electrokinetic injection. With ICP-MS detection an optimal internal standard, with the same electrophoretic mobility as the analyte, can be used.

Keywords: Interfaces, CE–MS; Capillary electrophoresis–mass spectrometry; Nebulizing interface; Instrumentation; Chromium; Alkali metals; Alkaline earth metals; Metals

1. Introduction

The aim of this study has been to develop an interface for the coupling of capillary electrophoresis (CE) and inductively coupled plasma mass spectrometry (ICP-MS). The combination of the high plate numbers and the speed of separation achieved by CE with the sensitive, element specific detection capabilities of ICP-MS is a promising instrumental set-up to meet the future challenges of element speciation.

The use of microflow separation techniques is interesting, due to the extremely low consumption of sample and solvent. Especially in the sample limited situations frequently encountered in biological, biomedical and nuclear research, CE and micro-liquid chromatography (LC) are interesting alternatives to traditional high-performance liquid chromatography (HPLC). In some cases, such as sampling from single biological cells, CE could be the only practical approach. As the trend to treat all solvent effluents as hazardous wastes continues, the use of microflow techniques is likely to gain further popularity [1–3].

Even though the small sample volumes and the low liquid flow-rates used in CE limits the sensitivity obtained with CE–ICP-MS, there are ways to counteract these limitations. Preconcentration factors in the range 10–1000 can be obtained [4–6], by e.g., using electrostacking. With isotachophoresis preceding CE separation, it is possible to increase the

*Corresponding author.

0021-9673/98/$ – see front matter
PII: S0021-9673(98)00708-0

concentration of the analyte 10^5–10^6 times within 45 s [7]. While band broadening effects cause a dilution factor of about 100 in HPLC, these effects are in general much smaller for CE separations [7].

The most broadly used detectors for CE are UV and fluorescence emission detectors. Unfortunately, the selectivity of these detectors is limited; for speciation studies, the use of a universal and element specific detector would be an advantage. Although the coupling of CE–mass spectrometry (MS) was reported 11 years ago [8] and has been the subject of review articles [9,10], the number of papers reporting the coupling of CE to ICP-MS remains limited [11–20]. The most obvious reason for this is the lack of commercially available interfaces specially designed for CE–ICP-MS. This is probably due to the complexity of the coupling: there are no commercial nebulizers available that work well at the low flows used in CE. The challenge is to achieve effective introduction of microflows from CE to the ICP-MS without excessive band broadening, while maintaining a complete electrical circuit. To obtain a complete electrical circuit, Olesik et al. [11] covered the CE capillary with silver paint and used a concentric, pneumatic nebulizer (Meinhard) for the introduction to the ICP-MS system. Later papers describe the use of an extra flow of electrolyte to complete the electrical circuit [12–20]. A number of sample introduction modes have been tested, including modified Meinhard nebulizers [11,13,16–18], the direct injection nebulizer (DIN) [12], the ultrasonic nebulizer (USN) [15], electrothermal vaporization (ETV) [14] as well as hydride generation [19,20] with the reaction manifold and the gas–liquid separator situated after the CE column. Mei et al. [21] used a microconcentric (MCN) and a pneumatic nebulizer for the coupling of CE to ICP-AES. The next step should, in our opinion, be to use new nebulizer technology exclusively designed for the nebulization of microflows, and that has been the focus of this study.

2. Experimental

2.1. Apparatus

2.1.1. CE–ICP-MS set-up

A Shimadzu (Columbia, MD, USA) Model LC-9A pump and a 1/32 in. Valco cross coupling (Houston, TX, USA) were connected to a Perkin-Elmer (Norwalk, CT, USA) SCIEX ELAN 5000 ICP-MS system via a laboratory-built microconcentric nebulizer (Fig. 1) (1 in.=2.54 cm). The ICP-MS system was controlled by an IBM PS/2 77 486 DX2 computer equipped with ELAN 5000 (Xenics) software. The preferred CE–ICP-MS set-up is shown in Fig. 2. A 25 cm×75 μm I.D.×150 μm O.D. fused-silica capillary (Polymicro Technologies, Phoenix, AZ, USA) was used for the connection of the Valco 1/32 in. cross coupling to the nebulizer. Graphite and vespel ferrules (Scantech, Sweden) were used to obtain tight coupling of the connections to the cross and the nebulizer. A 40 cm×20 μm I.D.×150 μm

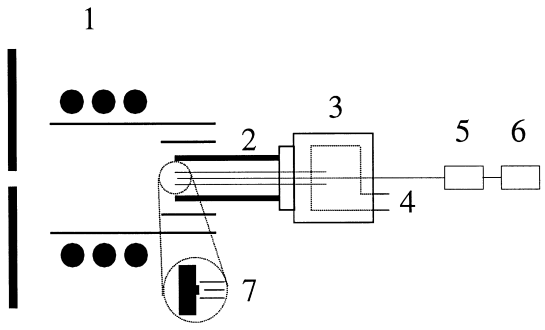

Fig. 1. Design of the microconcentric nebulizer. 1, ICP-MS sampler cone and torch; 2, ICP-MS injector liner; 3, nebulizer body; 4, nebulizer gas introduction; 5, HPLC pump; 6, mobile phase reservoir; 7, expanded view of liquid introduction capillary (inner), gas introduction capillary (outer) and a positioning tool.

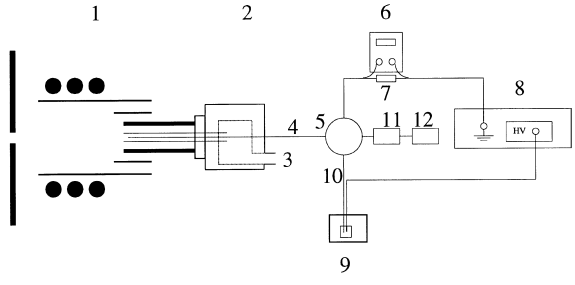

Fig. 2. CE–ICP-MS set-up. The electrical circuit is completed in front of the nebulizer using an extra flow of electrolyte. 1, ICP-MS sampler cone and torch; 2, nebulizer; 3, nebulizer gas inlet; 4, transfer capillary to ICP-MS system; 5, 1/32 in. cross; 6, multimeter; 7, 100 000 Ohm resistance; 8, high-voltage power supply; 9, CE inlet surrounded by plexi glass; 10, CE capillary; 11, HPLC pump; 12, extra electrolyte reservoir.

O.D. fused-silica capillary was used for the CE separations. The CE outlet was connected to the Valco cross along with the Pt grounding electrode. The high voltage inlet of the CE system was protected with a laboratory-built box made by Plexiglass. Electrokinetic injection (+30 kV, 10 s) was used and the separation voltage was +30 kV. The current was measured indirectly by a Multimeter 5318 CIE (Taiwan) as shown in Fig. 2 (item 6). The high-voltage power supply used was Brandenburg alpha III 3807 (West Midlands, UK).

2.1.2. Performance test of the nebulizer

In order to test the characteristics of different nebulizer designs, the LC pump was connected directly to the nebulizer by the use of a fused-silica capillary (Fig. 1). The mobile phase was 10 mmol l^{-1} HNO_3; Pb was added at a concentration of 200 μg l^{-1}. The X–Y position of the nebulizer tip was optimized to provide a maximal signal for Pb. The distance from the nebulizer tip to the ICP-MS plasma was about 5 mm, if not specified in the text. A specially designed tool (Fig. 1) was used to ensure the reproducible positioning of the two nebulizer capillaries.

2.1.3. ICP-MS parameters

The ICP-MS operating conditions and data acquisition parameters are given in Table 1. The following isotopes were measured: Na (m=23), Mg (m=24), K (m=39), Ca (m=43), Cr (m=52), Cd (m=114), Ba (m=138) and Pb (m=208). For the tests of sensitivity and precision using continuous sample introduction, 100 replicates and three consecutive measurements were used.

Table 1
ICP-MS operating parameters

Plasma gas flow-rate	15 l min^{-1}
Auxiliary	1.0 l min^{-1}
Nebulizer (variable)	0.8 l min^{-1}
Forward power	1000 W
Sampler	Ni, aperture diameter: 1.15 mm
Skimmer	Ni, aperture diameter: 0.89 mm
Injector liner	Alumina (2.0 mm I.D.)
Resolution	Normal
Data acquisition parameters	
Replicate time (ms)	500
Dwell time (ms)	500
Scanning mode	Peak hop
Sweeps/reading	1
Readings/replicate	1
Number of replicates	100–1200
Points/spectral peak	1

2.2. Reagents

The following reagents, all of analytical-reagent quality were obtained from Merck (Darmstadt, Germany): $CaCl_2 \cdot 5H_2O$, $MgCl_2 \cdot 6H_2O$, $CdCl_2$, $Pb(NO_3)_2$, $CrCl_3 \cdot 6H_2O$, K_2CrO_4, KCl, $BaCl_2 \cdot 2H_2O$ and HNO_3. $CuSO_4 \cdot 5H_2O$ (analytical reagent) was obtained from BDH (Poole, UK). Silver and copper paint were purchased from ELFA (Stockholm, Sweden). α-Hydroxyisobutyric acid (HIBA, puriss) and NaCl (analytical-reagent grade) were purchased from Fluka (Buchs, Switzerland). 4-Methylbenzylamine (UVCAT-1) was obtained from Waters (MA, USA). The CE electrolyte was 5.0 mmol l^{-1} UVCAT-1 and 6.5 mmol l^{-1} HIBA. Electrolytes and samples were filtered through 0.45-μm mixed cellulose esters–poly(vinyl chloride) (PVC) filters (Millex SLHA 025 BS) obtained from Millipore (MA, USA). Nafion cation-exchange membranes were obtained from Perma Pure (NJ, USA).

3. Results and discussion

3.1. Nebulizer development

The nebulizers used previously for the coupling of CE to ICP-MS were originally constructed to handle liquid flow-rates from 15 μl min^{-1} (DIN) to about 1 ml min^{-1}. In the case of the DIN nebulizer, signal pulsing occurs at liquid flow-rates lower than 15 μl min^{-1}, but there is little information in the literature about the possible causes for this behaviour and how to solve the problem. A complete solution of this problem is not given in this paper, but a couple of relevant results are presented.

In an earlier work [22], a microconcentric nebulizer was designed for the nebulization of organic solvents at liquid flow-rates lower than 10 μl min^{-1}. The nebulizer used a gas introductory capillary with an inner diameter (I.D.) of 0.5 mm. The liquid introductory capillary was situated in the centre of the nebulizer gas introductory capillary with the end of the liquid introductory capillary withdrawn 0.2

mm relative to the tip of the nebulizer gas introductory capillary. In this work, the same set-up (Fig. 1) was tested for the continuous nebulization of aqueous solutions. It was found that the signal for Pb (200 μg l^{-1} Pb, 10 mmol l^{-1} HNO_3) was much lower than expected from the results obtained previously for tetraalkyllead species in organic solvents [22]. The signal depression was probably caused by the less effective nebulization of the aqueous solutions. The surface tension is higher for water than for the organic solvents used in the earlier experiments. Therefore, the formation of larger droplets is expected, compared to the nebulization of organic solvents.

In order to obtain a more efficient aerosol formation, gas introduction capillaries with smaller inner diameters had to be used. Nebulizer gas introduction capillaries with I.D.s of 500 μm, 320 μm and 220 μm, and liquid introduction capillaries with I.D.s of 20 μm, 50 μm and 75 μm (all of 150 μm outer diameter) were tested. The use of a gas introduction capillary with I.D.=220 μm provided the highest sensitivity. The signal was a factor of 50 higher than with the use of a gas introduction capillary with I.D.=500 μm. No significant difference in sensitivity was observed between liquid introduction capillaries of different inner diameters. The nebulizer is shown in Fig. 1. The tip of the nebulizer gas introduction capillary (I.D. 220 μm) was placed on level with the original ICP-MS injector liner. Due to the small difference between the I.D. of the nebulizer gas capillary and the O.D. of the liquid introduction capillary, a nebulizer gas pressure of about 18–22 bar was needed to achieve a gas flow-rate of 800–850 ml min^{-1}. Because the ICP-MS gas supply system only allows a gas pressure of about 5 bar, an external nebulizer gas supply was used.

Two different designs of the nebulizer, as shown in Fig. 3, were tested. In design 1, the tip of the liquid introductory capillary was withdrawn about 1 mm relative to the nebulizer gas capillary tip. It was difficult to measure this distance exactly and the tool described in Fig. 1 could not be used for nebulizer gas capillaries with an inner diameter less than 500 μm. In design 2 the tip of the liquid introduction capillary was extended 1 mm beyond the tip of the gas introduction capillary. The two designs were found to be quite different with regard to the liquid flow-rate working range.

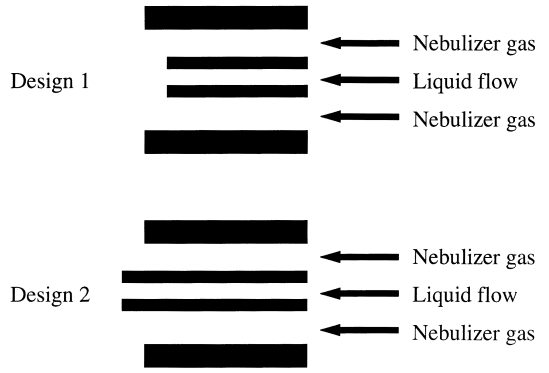

Fig. 3. The tip of the nebulizer for designs 1 and 2, respectively.

Only design 1 worked well in the range 1–7 μl min^{-1}, but at higher liquid flow-rates the plasma was quenched. The sensitivity increased linearly with increasing liquid flow-rate (Fig. 4). The precision was 3.3–5.3% relative standard deviation (R.S.D.) for measurements of 200 μg l^{-1} Pb in 10 mmol l^{-1} HNO_3 for liquid flow-rates in the range 1–7 μl min^{-1}. As illustrated in Fig. 5, signal pulsing was observed at the lowest nebulizer gas flow-rate (520 ml min^{-1}). The sensitivity increased with increasing nebulizer gas flow-rate in the range 520–840 ml min^{-1}.

Design 2 (Fig. 3) was found to work well in the range 9–15 μl min^{-1}. Below 9 μl min^{-1} we observed strong signal pulsing which was not removed by increasing the nebulizer gas flow-rate, unlike design 1. The sensitivity increased almost linearly with increasing liquid flow-rate as shown in Fig. 4. The precision was better than 1.0% R.S.D. for

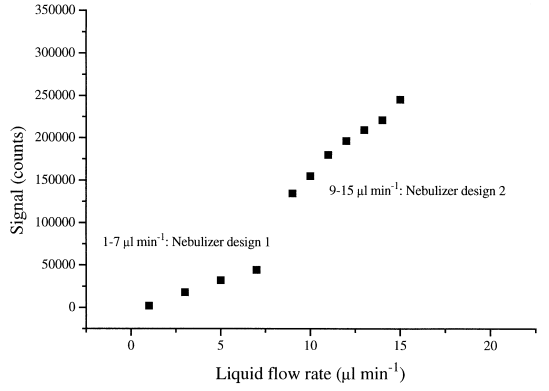

Fig. 4. The sensitivity as a function of the liquid flow-rate for continuous sample introduction.

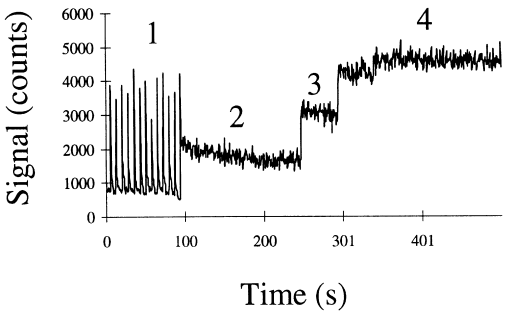

Fig. 5. Signal pulsing at low liquid flow-rates (2.5 μl min^{-1}) for nebulizer design 1. The nebulizer gas flow-rates were: 1, 520 ml min^{-1}; 2, 650 ml min^{-1}; 3, 780 ml min^{-1}; 4, 840 ml min^{-1}.

measurements of 200 μg l^{-1} Pb in 10 mmol l^{-1} HNO_3 for liquid flow-rates in the range 9–15 μl min^{-1}.

3.2. Design of the extra flow interface for the coupling of CE–ICP-MS

The use of an extra flow of electrolyte to complete the electrical circuit has been discussed in several papers concerned with the coupling of CE to MS and ICP-MS [12–20]. In Fig. 2, the electrical circuit is completed in front of the nebulizer (item 2) and a 25 cm transfer capillary (item 4) is used from the cross (item 5) to the tip of the nebulizer. To minimize sample dispersion effects (dilution and loss of resolution) and to avoid too high flow-rates into the CE capillary, the rate of the extra flow was kept as low as 2.5 μl min^{-1}. Therefore design 1 (Fig. 3) of the nebulizer, which was suitable for liquid flow-rates in the range 1–7 μl min^{-1}, was used. The extra flow of electrolyte (Fig. 2, items 11 and 12) introduced at the cross in front of the nebulizer transports the CE effluent from the cross to the nebulizer tip via a transfer capillary (Fig. 2, item 4). A fraction of this flow enters the CE capillary (Fig. 2, item 10), and this flow (V_{CE}) should be as small as possible. According to Eq. (1) [23], this means that the flow of extra electrolyte into the cross (V_{cross}) must be low:

$$V_{CE} = V_{cross}(d_{CE}/d_T)^4(L_T/L_{CE}) \quad (1)$$

where d_{CE} is the inner diameter of the CE capillary; d_T is the inner diameter of the transfer capillary; L_{CE} is the length of the CE capillary and L_T is the length of the transfer tubing.

The flow of extra electrolyte from the cross into the CE capillary is directed towards the injection end. For obvious reasons this flow must not be larger than the electrophoretic flow-rate of the analytes, which is directed towards the detection end of the CE capillary. Therefore, there is a maximum upper limit for the flow-rate of the extra electrolyte. For liquid flow-rates above the critical value, the analytes will be pushed back into the buffer reservoir at the inlet end of the CE capillary.

The set-up used is an analogue to the flow counterbalanced CE set-up described by Culbertson and Jorgenson [24]. They also give an equation for the additional band broadening (σ^2) due to the pressure-induced parabolic flow profile:

$$\sigma^2 = d_{CE}^2 v_{pa}^2 t/96D \quad (2)$$

where v_{pa} is the pressure-induced average flow-rate, t is the time occupied in the CE capillary and D is the analyte diffusion coefficient. To avoid extra band broadening effects due to the pressure-induced counterflow through the CE capillary, v_{pa} should be as low as possible. However, the sensitivity of the system decreases with decreasing liquid flow-rates (Fig. 4). Therefore, the choice of liquid flow-rate must be a compromise between the resolution of the separation and the sensitivity of the system. A flow-rate of 2.5 μl min^{-1} into the cross was found to work satisfactorily. However, when the high voltage was switched off, the net liquid flow was from the outlet end of the CE capillary towards the inlet end.

3.3. Figures of merit for the CE–ICP-MS coupling

In order to test the suitability of the CE-ICP-MS system, a mixture of Na^+, K^+, Ca^{2+}, Mg^{2+} and Ba^{2+} was analysed. The CE electrolyte was 6.5 mmol l^{-1} HIBA and 5.0 mmol l^{-1} UVCAT-1, which had previously been used for the determination of the same cations with indirect UV detection [25]. Therefore it was possible to compare the resolution and the detection limits obtained with CE–ICP-MS (post-column detection) and CE–UV (on-column detection). Before the run, the CE capillary was flushed with electrolyte by applying pressure at the injection end of the capillary. Due to the pressure-induced flow towards the injection end of the CE capillary, electrokinetic injection [26–28] had to be used.

A mixture of 2 mg l^{-1} K, Na, Ca, Mg and Ba was injected. The electropherogram is shown in Fig. 6. The responses of Na ($m=23$) and Ca ($m=43$) were omitted due to the low signal-to-noise ratios caused by the high background signal for these isotopes. As can be seen from Fig. 6, the peaks of K (2.0 min), Ba (2.5 min) and Mg (3.0 min) are well separated. The resolution factors (R_s) were calculated according to Eq. (3):

$$R_s = (2\ln 2)^{1/2}[\Delta t/(t_{1w1/2} + t_{2w1/2})] \quad (3)$$

where Δt is the difference between the migration times of the two analytes; $t_{1w1/2}$ and $t_{2w1/2}$ are the peak widths at half peak height for analytes 1 and 2, respectively [29]. For the separation of K and Ba the resolution factor was 1.9 and for Ba and Mg it was 2.0 ($R_s \geq 1.5$ indicates baseline separation). The resolution was a factor of five lower than with on-column indirect UV detection of the same elements using the same CE electrolyte. Due to the higher mobility of the analytes compared to the CE buffer co-ion, the peaks were fronting [30–32]. The limit of detection [$S/N=3$, the noise, N, was estimated from the baseline with 20 replicates (Table 1)] was estimated to be 0.9 mg l^{-1} for K, 10 μg l^{-1} for Ba and 0.3 mg l^{-1} for Mg. The sensitivity could be increased by using a longer injection time.

The same CE–ICP-MS set-up was also tested for the determination of Cr(III) in the presence of Cr(VI). Because the Cr(VI) specie is negatively charged (CrO_4^{2-}), it is separated from Cr(III) already at the point of injection. Cd(II) was used as internal standard in this experiment. As can be seen from Fig. 7, the Cr(III) (2.9 min) and Cd(II) (2.7 min) species have similar electrophoretic mobility ($R_s=0.84$), which makes Cd(II) particularly suitable as internal standard (see below). The constant Pb signal in Fig. 7 was used to monitor the nebulizer performance. The instrumental detection limit [$S/N=3$, the noise, N, was estimated from the baseline with 20 replicates (Table 1)] was found to be 10 μg l^{-1} for Cr(III) and 3 μg l^{-1} for Cd(II). The reproducibility of the migration times was 0.6% R.S.D. ($n=4$) for Cr(III) and Cd(II). The precision for the determination of 250 μg l^{-1} Cr(III) in the presence of 150 μg l^{-1} Cr(VI) (standard solutions) was found to be 3.6% R.S.D. ($n=3$) using Cd(II) as internal standard.

An internal standard must be used for quantitative analysis: when the CE capillary is moved from the sample solution to the CE running electrolyte, some of the injected sample is lost, due to the reversed flow in the CE capillary when the high voltage is off.

3.4. Ruggedness of the CE–ICP-MS interface compared to alternative interface designs

A number of alternative CE–ICP-MS interface designs were tested with mostly negative results. We have included a brief description below, to the benefit of CE–ICP-MS beginners.

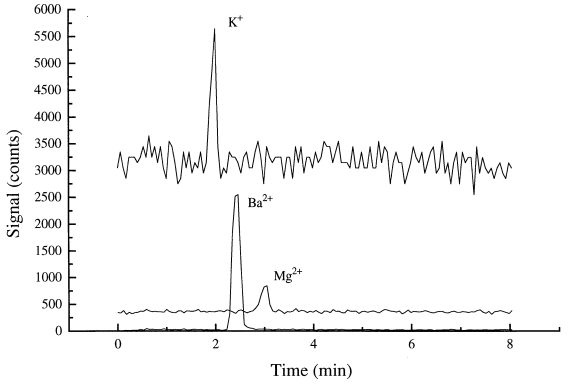

Fig. 6. CE–ICP-MS electropherograms. Sample, 2 mg l^{-1} of K, Mg and Ba; CE electrolyte, 6.5 m*M* HIBA and 5.0 m*M* UVCAT-1; injection, +30 kV (10 s); separation voltage, +30 kV (0.8 μA).

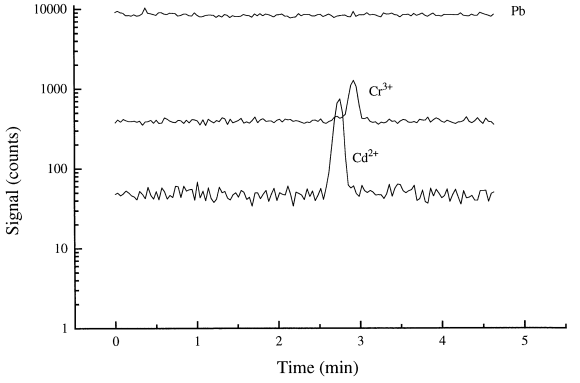

Fig. 7. CE–ICP-MS electropherograms. Sample, 250 μg l^{-1} of Cr(III), 150 μg l^{-1} Cr(VI) and 160 μg l^{-1} Cd(II); CE electrolyte, 6.5 m*M* HIBA and 5.0 m*M* UVCAT-1; injection, +30 kV (10 s); separation voltage, +30 kV (0.9 μA). The signal from 200 μg l^{-1} Pb was included to monitor the nebulizer performance.

An approach, where the electrical circuit was completed by the use of an extra flow of electrolyte to the tip of the nebulizer, was tested. However, due to the short distance (5 mm) between the CE terminus and the radio frequency (RF) coil of the ICP-MS, the high voltage used for the CE run interfered with the RF supply to the plasma: the plasma was extinguished as soon as the CE high voltage was switched on. This also happened when the tip of the CE capillary was placed in intermediate positions between the cross and the tip of the nebulizer. In principle, the tip of the nebulizer could be placed at a longer distance from the plasma, but this would decrease the sensitivity significantly, due to lower aerosol transport efficiency.

Interfaces including the use of conductive paint (silver and copper) at the tip of the CE capillary were also tested. In these experiments, the distance from the tip of the nebulizer to the plasma was increased to 11.5 cm in order to sustain the plasma when the CE high voltage was switched on. It was found that the electrical circuit was disrupted during the runs, probably because of deterioration of the conductive paint due to electrochemical effects.

The design described by O'Shea et al. [33] was tested (an electrochemical detector was used in their work), by making a crack [33] in the CE capillary through which the electrical circuit was completed: the crack was surrounded by an electrolyte. However, the analyte leaked out of the crack even when the crack was covered with a Nafion ion-exchange membrane. The CE capillary broke very easily at the point of the crack.

Therefore, due to the lack of ruggedness, the other interface designs were abandoned.

3.5. Removal of the electrokinetic injection bias by the use of an internal standard

The matrix effects associated with the use of electrokinetic injection are well documented [26–28]. However, if the internal standard has the same electrophoretic mobility as the analyte, no injection bias should be observed. Because the ICP-MS system is an isotope specific detector, the internal standard can co-migrate with the analyte specie. This approach is difficult to use with UV or fluorescence detection. Thus, with the coupling of CE and ICP-MS, a unique correction method for injection bias is available. As can be inferred from Fig. 7, Cd(II) is a suitable internal standard for the determination of Cr(III).

4. Conclusions

The ideal coupling of CE to ICP-MS would feature high sensitivity and high electrophoretic resolution. The proposed CE–ICP-MS set-up is a compromise between the two properties. An extra flow of electrolyte completed the electrical circuit, and a special microconcentric nebulizer was used for sample introduction. Electrokinetic injection was used, because it provides a higher sensitivity and also higher electrophoretic resolution than other injection techniques. The matrix effects normally experienced with this injection method can be corrected by the use of an internal standard with the same electrophoretic mobility as the analyte.

Acknowledgements

The authors thank NorFA for the financial support of A.T.'s stay at Stockholm University, Sweden.

References

[1] M. Guardia, J. Ruzicka, Analyst 120 (1995) 17N.
[2] H.B. Wan, M.K. Wong, J. Chromatogr. A 754 (1996) 43.
[3] C. Ericson, S. Hjerten, Anal. Chem. 70 (1998) 366.
[4] L. Chien, D. Burghi, J. Chromatogr. 559 (1991) 141.
[5] S. Palmarsdottir, L.E. Edholm, J. Chromatogr. A 693 (1995) 131.
[6] C. Zhang, W. Thormann, Anal. Chem. 68 (1996) 2523.
[7] P. Jandik, G. Bonn, Capillary Electrophoresis of Small Molecules and Ions, VCH, New York, 1993, pp. 118–119.
[8] J.A. Olivares, N.T. Nguyen, C.R. Yonker, R.D. Smith, Anal. Chem. 59 (1987) 1230.
[9] R.D. Smith, J.H. Wahl, D.R. Goodlett, S.A. Hofstadler, Anal. Chem. 65 (1993) 574A.
[10] J. Cai, J. Henion, J. Chromatogr. A 703 (1995) 667.
[11] J.W. Olesik, J.A. Kinzer, S.V. Olesik, Anal. Chem. 67 (1995) 1.
[12] Y. Liu, V. Lopez-Avila, J.J. Zhu, D.R. Wiederin, W.F. Beckert, Anal. Chem. 67 (1995) 2020.
[13] Q. Lu, S.M. Bird, R.M. Barnes, Anal. Chem. 67 (1995) 2949.

[14] B. Michalke, P. Schramel, J. Chromatogr. A 750 (1996) 51.
[15] Q. Lu, R.M. Barnes, Microchem. J. 54 (1996) 129.
[16] J.A. Kinzer, J.W. Olesik, S.V. Olesik, Anal. Chem. 68 (1996) 3250.
[17] B. Michalke, P. Schramel, Fresenius J. Anal. Chem. 357 (1997) 594.
[18] B. Michalke, S. Lustig, P. Schramel, Electrophoresis 18 (1997) 196.
[19] M.L. Magnuson, J.T. Creed, C.A. Brockhoff, J. Anal. Atom. Spectrom. 12 (1997) 689.
[20] M.L. Magnuson, J.T. Creed, C.A. Brockhoff, Analyst 122 (1997) 1057.
[21] E. Mei, H. Ichihashi, W. Gu, S. Yamasaki, Anal. Chem. 69 (1997) 2187.
[22] A. Tangen, R. Trones, T. Greibrokk, W. Lund, J. Anal. Atom. Spectrom. 12 (1997) 667.
[23] J. Tehrani, R. Macomber, L. Day, J. High. Resolut. Chromatogr. 14 (1991) 10.
[24] C.T. Culbertson, J.W. Jorgenson, Anal. Chem. 66 (1994) 955.
[25] A. Tangen, W. Lund, R.B. Frederiksen, J. Chromatogr. A 767 (1997) 311.
[26] X. Huang, M.J. Gordon, R.N. Zare, Anal. Chem. 60 (1988) 375.
[27] E.V. Dose, G.A. Guiochon, Anal. Chem. 63 (1991) 1154.
[28] T.T. Lee, E.S. Yeung, Anal. Chem. 64 (1992) 1226.
[29] T. Manabe, N. Chen, S. Terabe, M. Yohda, I. Endo, Anal. Chem. 66 (1994) 4243.
[30] F.E.P. Mikkers, F.M. Everaerts, Th.P.E.M. Verheggen, J. Chromatogr. 169 (1979) 1.
[31] F.E.P. Mikkers, F.M. Everaerts, Th.P.E.M. Verheggen, J. Chromatogr. 169 (1979) 11.
[32] S. Hjerten, Electrophoresis 11 (1990) 665.
[33] T.J. O'Shea, R.D. Greenhagen, S.M. Lunte, C.E. Lunte, M.R. Smyth, D.M. Radzik, N. Watanabe, J. Chromatogr. 593 (1992) 305.